Geofísica Internacional (1996), Vol. 35, Num. 3, pp. 329-338

Lithospheric stress state in South America as inferred from tidal triggering of earthquakes

Alexei Nikolaev[1] and Vsevolod Nikolaev[2]
[1] *Research and Coordinating Center for Seismology and Engineering RAS, Moscow, Russia.*
[2] *Institute of Physics of the Earth RAS, Moscow, Russia.*

RESUMEN

Se presenta un modelo del estado de esfuerzo en la litosfera sudamericana, con base en el desgatillamiento de sismos por efecto de las mareas. Se utilizó un catálogo de 23,399 temblores de magnitud M>3.5 y se calculó la diferencia entre el número de temblores que ocurre durante fases opuestas de la marea. Se calcularon los coeficientes de Lode-Nadai, que muestran el estado de esfuerzo tensional a lo largo de la Cordillera, y caótico en el interior del continente.

PALABRAS CLAVE: Esfuerzo de mareas, efecto de gatillo, Sudamérica.

ABSTRACT

We present a model for the lithospheric stress state in South America inferred from tidal triggering of earthquakes. The South American plate is attractive for study because the slab pull component should be small and the other components are reasonably isolated geographically.

A catalogue of South America earthquakes which contains 23,399 events with M>3.5 has been used for the study of the Earth tide triggering effect. The normalized difference, t, between the number of shocks occurring during positive and negative phases of tidal vector components is used to estimate the tidal triggering effect. This value t has a mosaic spatial distribution and changes with time.

The tidal triggering effect is also connected with a few harmonic components of the Earth tide that differ from area to area.

We present maps of the Lode-Nadai coefficient, that characterizes the lithosphere stress state. These maps show a dominant state of tension along the Cordilleras and a rather chaotic distribution in the inner-continental area. The detailed features have a complex character and are not distinctly tied with tectonic elements.

The maps of the orientation of compression and tension axes are also obtained using a tidal triggering effect.

KEY WORDS: Tidal stress, triggering, South America.

INTRODUCTION

The fine structure of seismicity can be affected by earth tides (Nikolaev, Nikolaev, 1993a, 1993b; Nikolaev, 1993). There have been several attempts to study these effects, but as far as we know, their results are rather contradictory and unstable both spatially and temporally (Heaton, 1975; 1982, De Freitas *et al.*, 1991; Knopoff, 1964). This study is oriented towards the regularities of seismicity's fine structure associated with earth tides. Earth tide stresses can be considered as a periodical loading of the Earth's crust that interferes with the background tectonic stress field. The background process can be due to the preparation of a strong earthquake, creep, and weak seismicity. Taking into account that the majority of earthquake sources result from movement along fault planes, one can consider three main types of fracture: normal, strike-slip and thrust. The earthquake triggering process depends both on slow background changes in the stress field and on comparatively short variations in earth tide stresses. Depending on the earth tide phase, tidal forces can either act towards the geodynamic process or opposite to it. Thus, it can either stimulate or suppress the triggering effect. Hence, the character of tidal stresses acting at the moment of an earthquake corresponds to that of the stress released by it. Therefore, the study of tidal phases in relation to the origin time of earthquakes allows us to solve the inverse problem, to find the character of stresses acting in the individual earthquake source, and the tendency and character of the stress field prevailing during a certain time interval and within a certain volume of the Earth's crust.

METHOD AND DATA

We used a world-wide Hudson catalogue containing 23,399 earthquakes of magnitude M>3.5 which occurred during 1966-1993. The study region lies between 30° and 85°W, and betweeen N10° and S60°, and is divided into 4x4 degrees windows as is shown in Figure 1a.

Algorithms are available to calculate earth tide characteristics for every geographical point and for every moment of time. This study makes use of Longman's algorithm (Longman, 1959). Figure 1a presents a map of the shallow (0-70 km) earthquake distribution in each window. Figure 2a presents a map of the deep earthquake (more 70 km) distribution in each window.

To study the tidal triggering effect, we use the following method. In every window we calculate the number of earthquakes which happened during the negative phase N_-, during the positive phase N_+, of components of the tidal

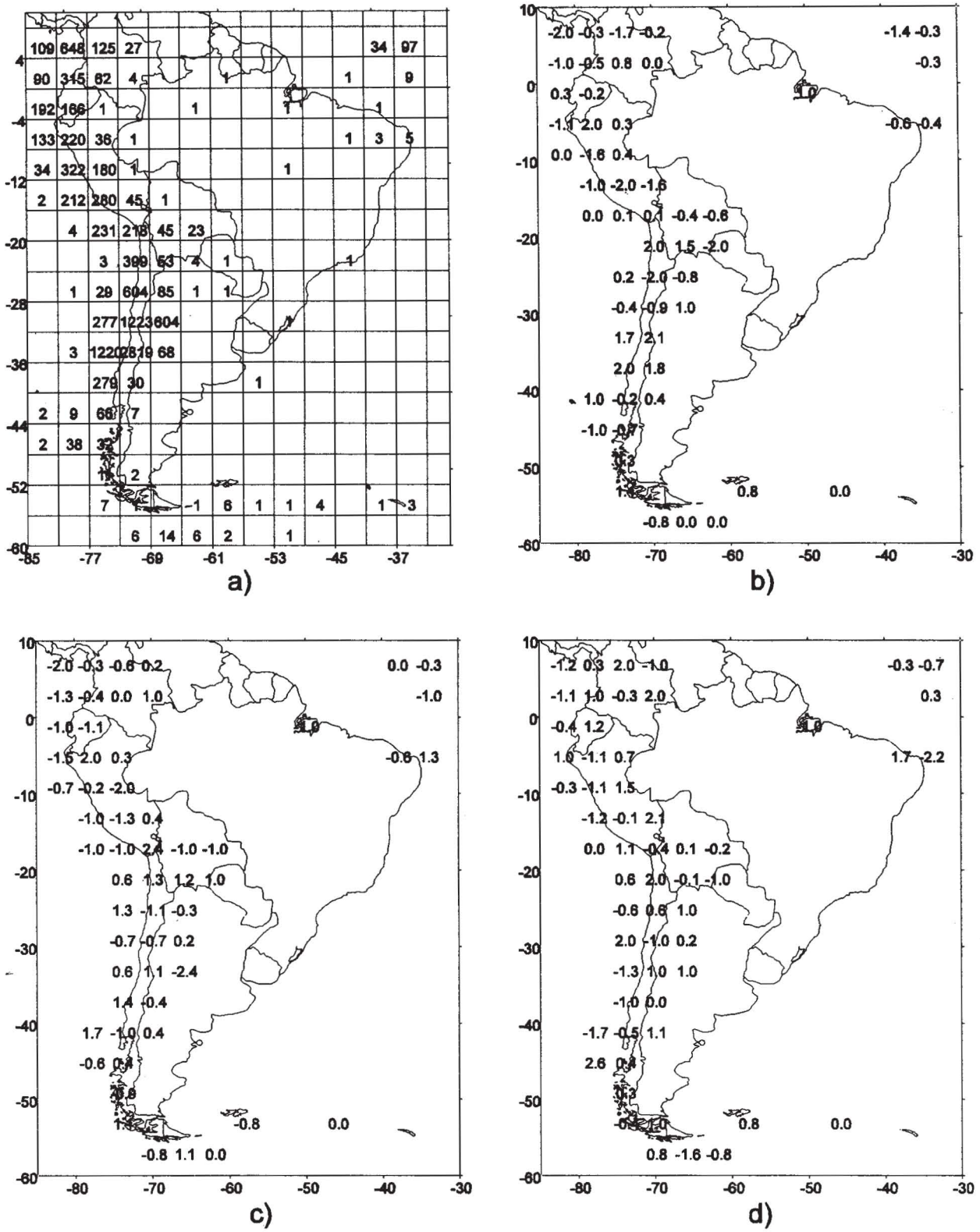

Fig. 1. a) Number of earthquakes occurring in 4x4 degrees windows during 1966-1993, depth 0-70 km. Standardized differences, t, of earthquakes occurring during negative and positive phases of the vertical (b), west-east (c) and north-south (d) component of the tidal vector.

vector (vertical, north-south and west-east). The positive phase is the increasing of tidal component from North to South, from East to West and from Down to Up. The difference between these numbers, $N_- - N_+$, can be considered

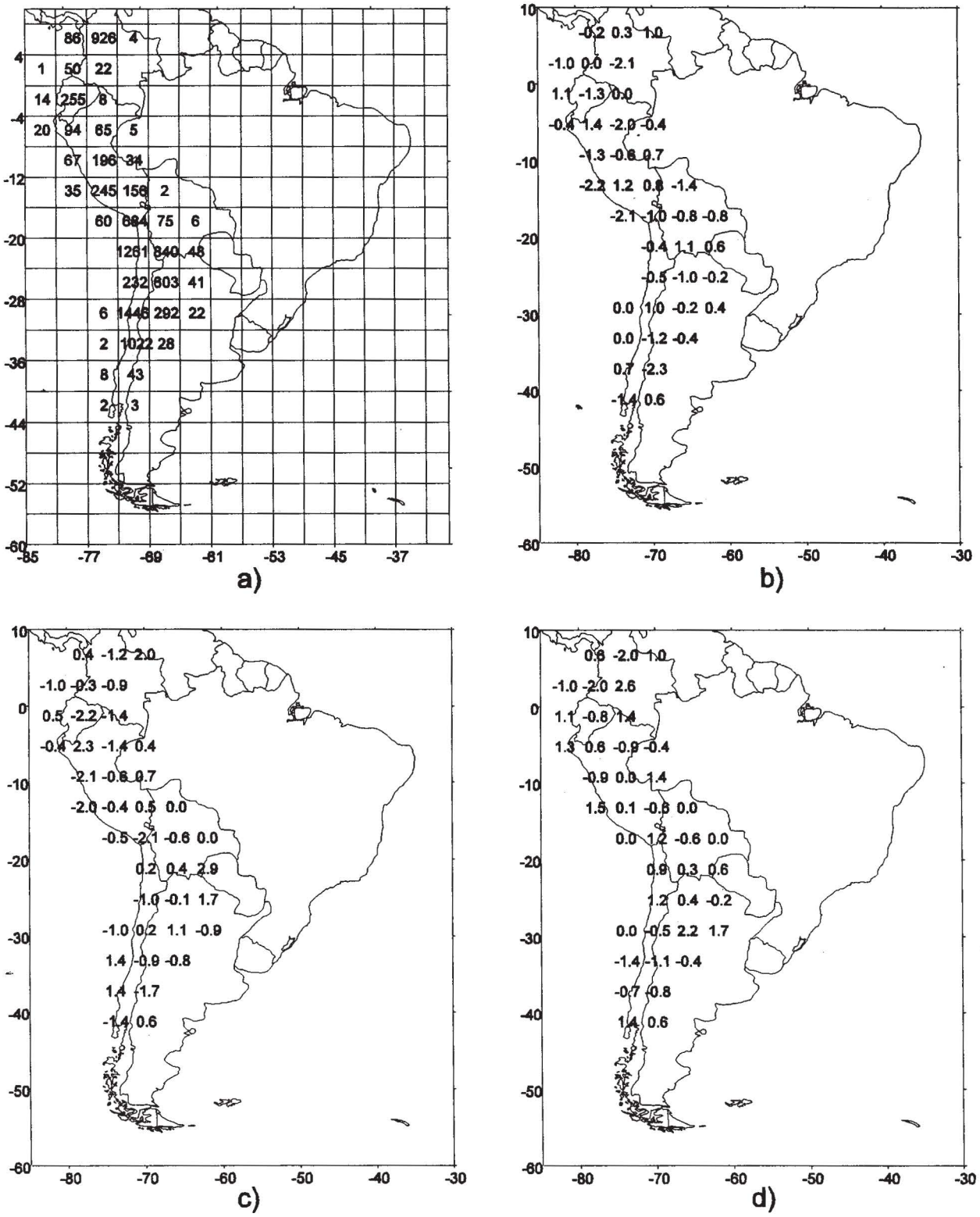

Fig. 2. a) Number of earthquakes occuring 4x4 degree windows during 1966-1993, depth more than 70 km. Standardized differences, t, of earthquakes occurring during negative and positive phases of the vertical (b), west-east (c) and north-south (d) component of the tidal vector.

a consequence of the tidal triggering effect if it is statistically confident. From the statistical point of view, more informative is the characteristic of the normalized difference,

$$t = \sum (N_- + N_+)/2\sigma_N \quad ,$$

where σ_N is the standard deviation of the mean value $(N_- - N_+)/2$. For the binomial distribution of N_- and N_+, the

standard deviation is given by

$$\sigma = pq\sqrt{(N_- + N_+)} \quad ,$$

where p and q are the probability for an event to occur during the phase of tidal compression and tidal tension, respectively. If the earthquake occurrence times are independent of the tide phase, p=q=0.5. So we can verify the hypothesis of nonrandom difference N_- -N_+. If the module of the normalized value t is significant, equal to 1.5 or more, this should be considered to be a manifestation of the tidal triggering effect.

This statistical approach is a variant of Schuster test (Heaton, 1982), only with two sectors: 0-180 and 180-360 degrees. Our approach is more simple and convenient for spatial visualization (Figure 1b,c,d) and interpretation.

Figure 1b,c,d show the maps of normalized differences, t, for earthquakes that occurred during different phases of tidal component. For example, Figure 1b shows a triggering effect of earthquakes for the vertical tidal component: 7 windows out of 54 (13%) have t value that exceeds two standard deviations. The result evidences a tidal triggering effect. Similar results can be seen in Figure 1c for the west-east tidal component and on Figure 1d for the north-south tidal component. The areas characterized by a similar response of the tidal force (positive or negative) are clustered and form rather large areas stretching up to 1500-2000 km. This regularity is considered to be independent evidence of a nonrandom character of the t-value.

Figure 2b,c,d show the spatial distribution of t-values for earthquakes occuring at depths of more than 70 km. For example, Figure 2c shows a triggering effect of earthquakes for the west-east tidal component: 7 windows out of 41 (17%) have t value that exceeds two standard deviations. This result evidences a tidal triggering effect. Similar results, but not so strong, can be seen in Figure 1b for the vertical tidal component and in Figure 1d for the north-south tidal component. The areas characterized by a similar response of the tidal force (positive or negative) are clustered and form rather large areas stretching up to 1500-2000 km.

To verify the hypotheses about nonrandom distribution of t-values, we correlated the t-values calculated during two temporal intervals: 1966-1978 and 1979-1993 (for shallow earthquakes). The coefficients of correlation vary from 0.27 (vertical component) to 0.41 (west-south component). This correlation evidences both the existence of tidal triggering and its temporal changes.

Temporal variations of correlation between regional seismicity and tidal phases

To investigate temporal variations of the correlation between seismicity of the South America region and tidal phases, an analysis was made of the spectral-temporal diagram of the distribution of cumulative standard differences in the number of earthquakes both in the negative and positive phases for separate tidal waves and components (Figure 3a- for depth 0-70 km; Figure 3b- for depth of more than 70 km). Time, corresponding to the center of a sliding non overlapping time-window of 6 months, is marked on the horizontal axis of the diagram, individual tidal waves with periods from 8 hours to 6 months are indicated on the lower part of the vertical axis components of a tidal vector: module, vertical, north-south and eastwest (Nikolaev, 1994). The are indicated on the upper part of the vertical axis.

The intensity and locality of these zones evidence the domination of some tidal waves over others. At the same time, the domination of separate waves is traceable in different time intervals.

As is seen from the upper part of the diagram in Figure 3a, the shallow earthquakes dominate steadily in negative phases in the north-south direction during 1970-1985 and in negative phases in the vertical direction during 1967-1984.

As is seen from the upper part of the diagram in Figure 3b, the deep earthquakes dominate steadily in tensile phases in the north-south direction during 1985-1993.

There are intervals where the spectral structure changes (Figure 3b), for example in 1974-1976. These changes are expressed in the alteration of some dominating waves; in their junction and splitting. During 1966-1972, wave O1 is well seen but later damped. The main change in spectral structure falls during 1969-1971: waves Mf, O1, M1, which were statistically significant in tidal triggering until then, are damped and there appears: wave S1, which then dominates within 22 years as well as waves π1, M2, λ2. Splitting could also be derived: in 1977 wave Q1 splits from wave O1. The intervals of change in spectral structure are replaced by those of relative stability in 1976-1985.

The deep tidal triggering spectral structure (Figure 3b) is more simple, but the main dominating waves are the same - S1 (1966-1993). Generally, the influences of tidal waves in the deepest part of lithosphere may seem to be weaker.

So, the tidal triggering effect changes in time and it is significantly different for individual harmonic components. Even when the Earth's tide shows no impact on the seismicity, some tidal waves' influence is significant. Temporal changes in the tidal triggering effect show its high sensitivity to changes of the background stress field that is also demonstrated in spatial and temporal variations of seismicity. This is a manifestation of the Earth's lithosphere metastability as its fundamental property.

Lithospheric stress state in South America

We suppose that the tensoral sum of the tidal stress tensor calculated in small volumes of lithosphere at the

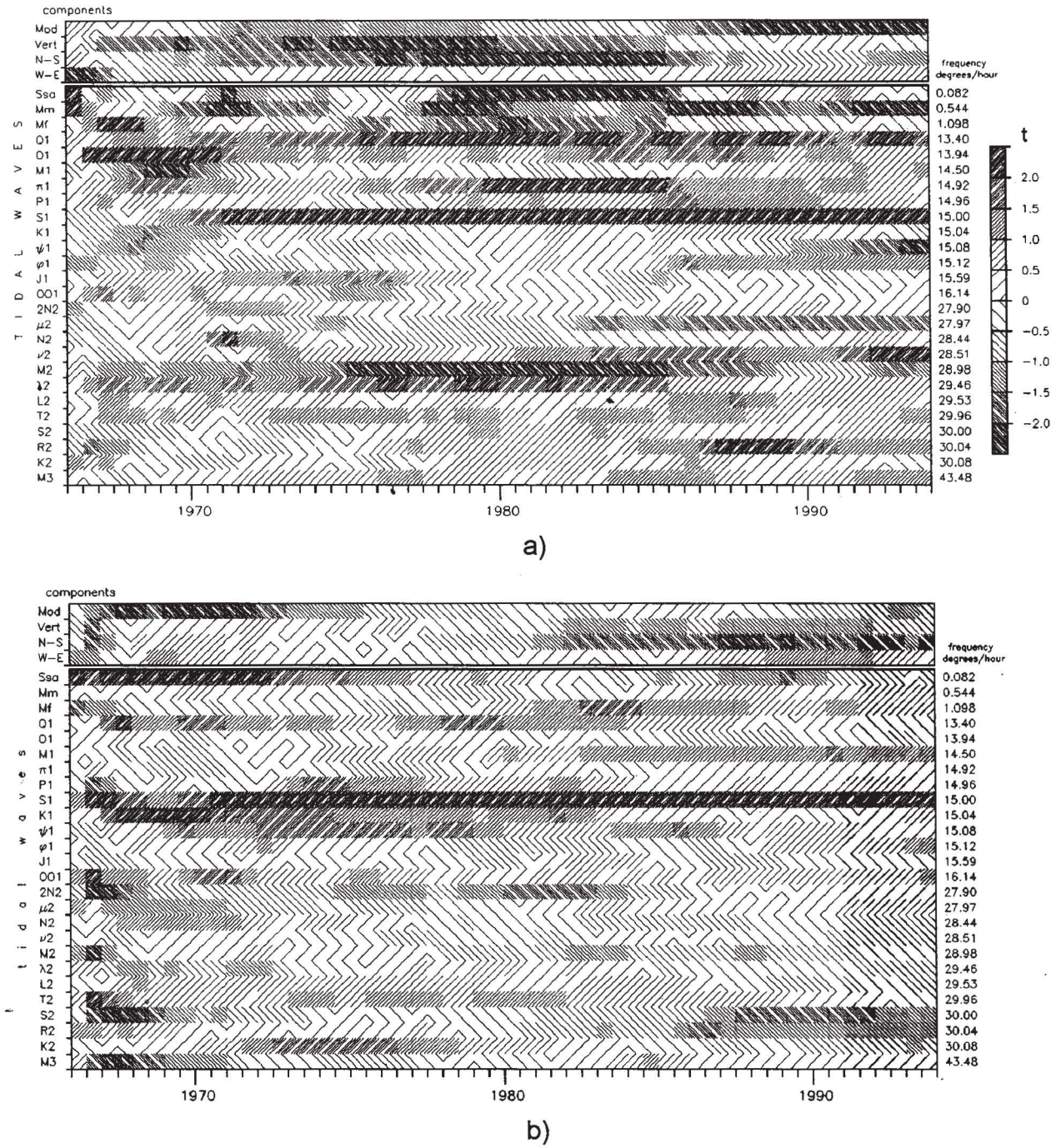

Fig. 3. Spectral-temporal diagram of earthquakes tidal triggering effect for separate tidal waves and components. South America 1966-1993; a) depth 0-70 km, b) depth >70 km.

moment of earthquakes is an indicator of the tectonic stress field.

To estimate the lithosphere stress state, we mapped the Lode-Nadai coefficient μ, where

$$\mu = 2\left(\frac{\sigma_2 - \sigma_3}{\sigma_1 - \sigma_3}\right) - 1 \quad ,$$

and where σ_1, σ_2, σ_2, are the main tidal stresses calculated at the origin time of earthquakes. If this coefficient is equal to -1, it corresponds to single-axis tension; if this coefficient is equal to 0, it corresponds to pure shear stress; if this coefficient is equal to +1, it corresponds to single-axis compression; if this coefficient is negative (-1 to 0) it conforms to general tension stress; if it is positive (0 to +1) it conforms to general compression stress. The coefficient μ

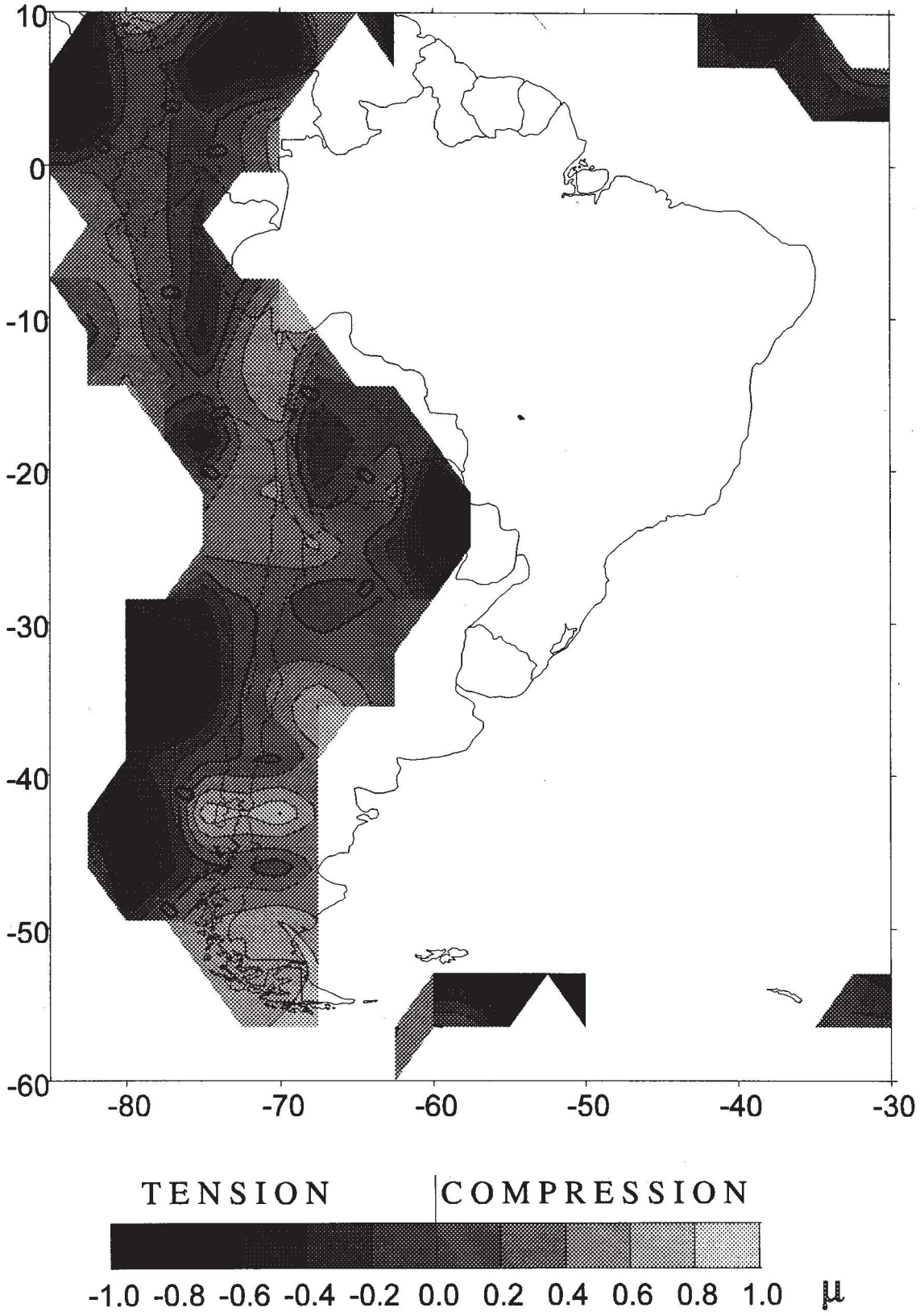

Fig. 4a. Map of Lode-Nadai coefficient inferred from correlation between tidal stress tensor and earthquake origin time during 1966-1993. Depth 0-70 km.

describes the general stress state and it is shown in Figure 4a,b. Generally, crustal tension predominates in the northern part of South America, from Columbia to Peru, and compression dominates in the southern part of the conti-

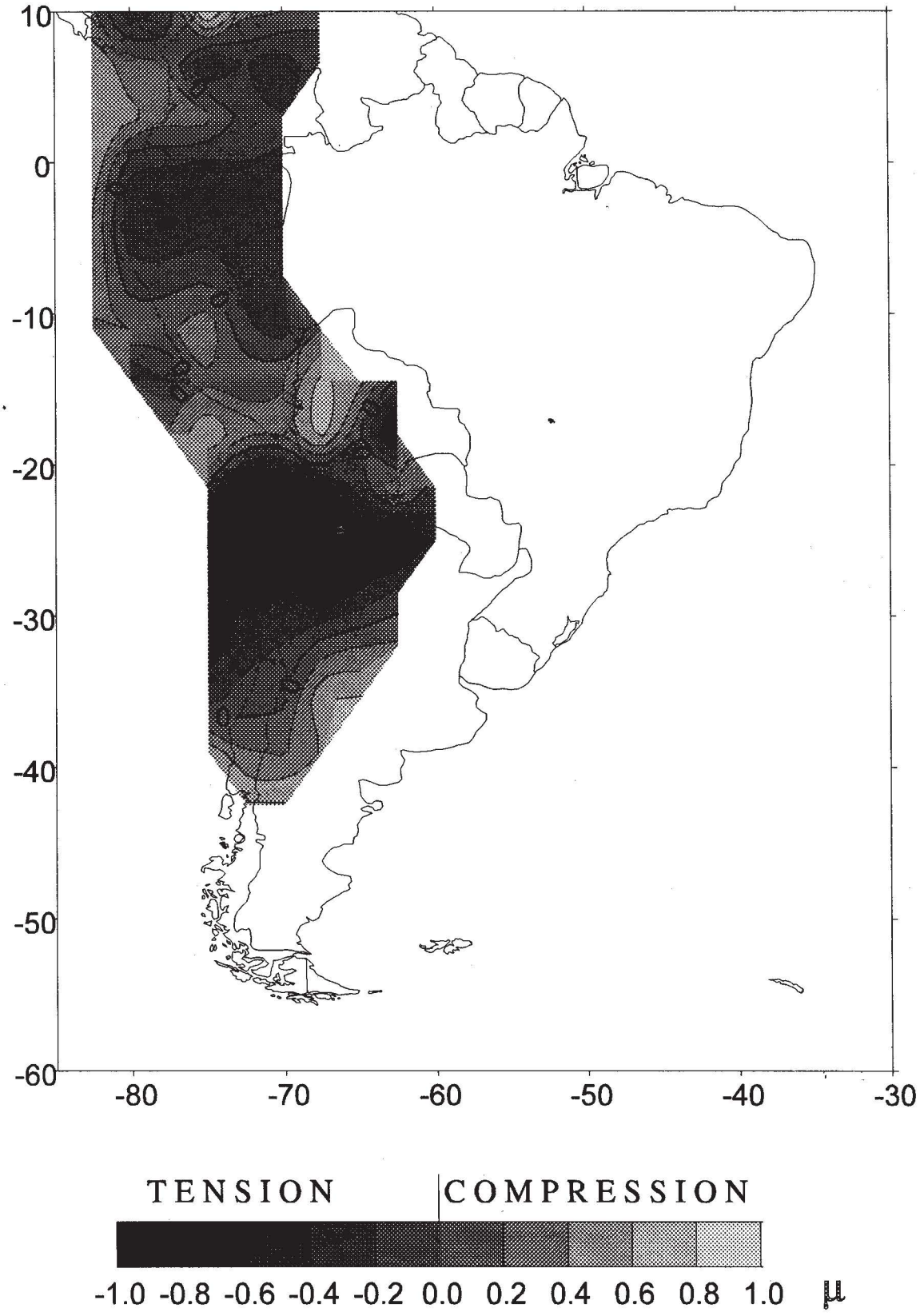

Fig. 4b. Map of Lode-Nadai coefficient inferred from correlation between tidal stress tensor and earthquake origin time during 1966-1993. Depth >70 km.

nent (Figure 4a). In the deeper parts of the lithosphere (Figure 4b), tension predominates in the central part from Chile to Bolivia, while compression predominates in the northern part of the continent.

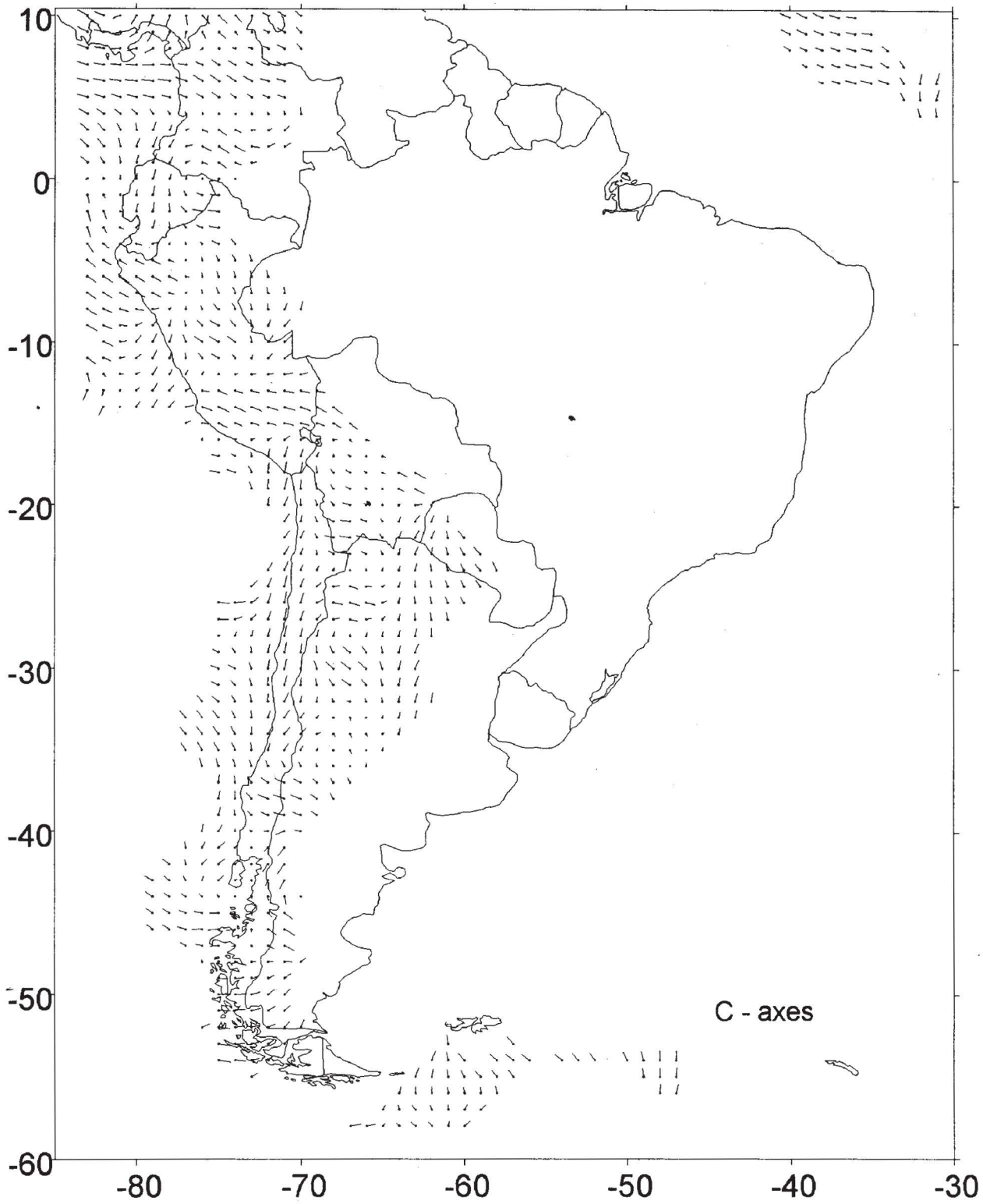

Fig. 5a. Orientation of compression axes calculated form correlation between tidal stress tensor and earthquake origin time; solid circles attached to the axes are on surface; axes show compressional stress direction under surface (lower hemisphere). 1966-1993. Depth 0-70 km.

For South America, compression oriented nearly E-W dominates, although there are clearly some complications such as in the Amazon basin and in the high Andes (Richardson, 1992). The western portion of the plate has nearly E-W compressive stress, though at altitudes greater than 3000-m stresses are extensional in an N-S direction (Stefanick and Jurdy, 1992).

Figure 5a,b show the orientation of compression and tension axes, respectively, calculated from correlation be–

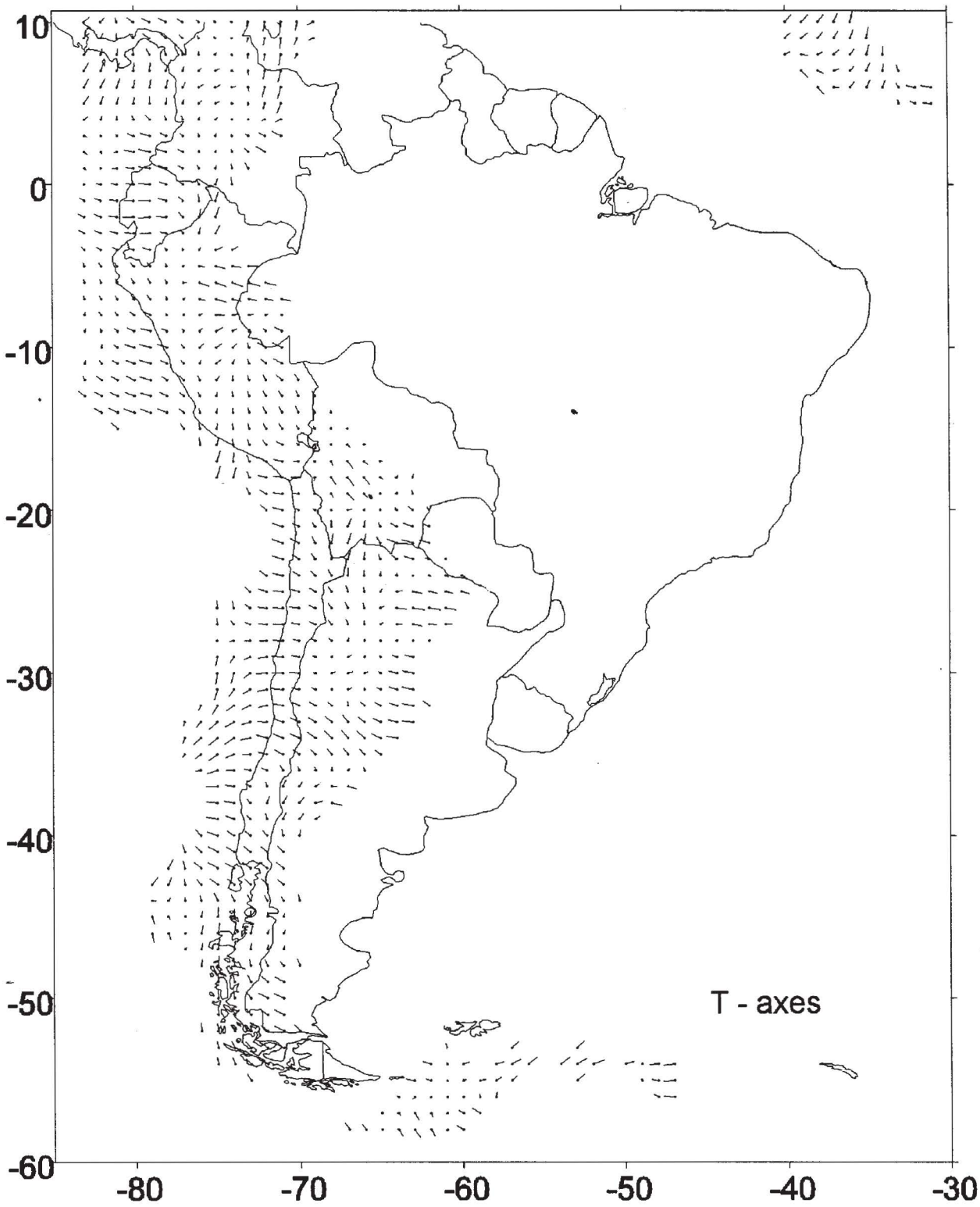

Fig. 5b. Orientation of tension axes calculated from correlation between tidal stress tensor and earthquake origin time; solid circles attached to the axes are on surface; axes show tensional stress direction under surface (lower hemisphere) 1966-1993. Depth 0-70 km.

tween tidal stress tensor and earthquake's origin time. The tensoral sum is calculated in 4x4 degrees windows. The field obtained is characterized by a complex structure with azimuth changes and whirlwinds. Generally, the orientation of compression axes in the upper part of the lithosphere coincides with the azimuth of the subduction zone (Figure 5a). Our stress map is more detailed than the well-known maps of Assumpcao (Assumpcao, 1992) that inferred stress from focal mechanisms of strong earthquakes, because we used a great number of moderate earthquakes.

CONCLUSIONS

Temporal and spatial distribution of the tidal triggering of earthquakes reveals triggering of moderate seismicity responses on the tidal phases. It forms rather large spatial anomalies stretching up to 2000 km. In terms of the stress state of lithosphere one should conclude that vertical and horizontal components of stresses are rather irregular and, in general, compression dominates over the tension.

A triggering effect is influenced differently by different harmonic components of the Earth's tide, and dominating regularities are different in space and time. The conclusion could be drawn that the triggering effect reflects not only the background state of the stress field, but also its tendency to change with time. The obtained dominant time intervals of tidal triggering changes are on the order of 10-20 years.

These results show that the real time tectonics displayed in the fine space and time structure of the stress field is more complex and different as compared with long-period tectonic regularities.

ACKNOWLEDGEMENTS

This research was supported by INTAS funds, Reference Number 93-1547.

BIBLIOGRAPHY

ASSUMPCAO, M., 1992. The regional interplate stress field in South America. *J. Geophys. Res., 97,* B8, 11889-11903.

De FREITAS, S.R.C., M. Van RUYMBEKE B. DUCARME and M. ASSUMPCAO, 1991. Correlation between Earth gravity tides and seismic activity at Joao Camara-Brazil. *In:* Proceedings of the Workshop: Geodynamical Instrumentation applied to Volcanic Areas. Luxembourg, 363-378.

HEATON, T.H., 1975. Tidal Triggering of earthquakes. *Geoph. J. of the Royal Astr. Soc., 43,* 307-326.

HEATON, T.H., 1982. Tidal Triggering of earthquakes. *Bull. Seism. Soc. Am., 72,* 6, 2181-2200.

KNOPOFF, L., 1964. Earth tides as triggering mechanism for earthquakes. *Bull. Seism. Soc. Am., 54,* 1865-1870.

LONGMAN, I.M., 1959. Formulas for computing the tidal accelerations due to the moon and sun. *J. Geophys. Res., 64,* 2351-2355.

NIKOLAEV, A.V. and V.A. Nikolaev, 1993a. Correlation between aftershocks of strong Earthquakes and tidal phases as indicator of stress state of media. Reports of Russian Academy of Sciences, 330, 2, 261-266, (in Russian).

NIKOLAEV, A. V. and V. A. Nikolaev,1993b. Earth's tides influence on the seismicity fine structure in the Ibero-Maghrebian region. *Física de la Tierra. Madrid, 5,* 71-76.

NIKOLAEV, V.A., 1993. Tidal triggering of earthquakes as indicator of lithosphere stress state in Mediterranean. European Geoph. Soc. *Annales Geophysicae, 1,* 66.

NIKOLAEV, V.A., 1994. Correlation between seismicity and phases of separate tidal waves. *Reports of Russian Academy of Sciences. 336,* 3, 98-10 (in Russian).

STEFANICK, M. and D.M. JURDY, 1992. Stress observations and driving force models for the South American plate. *J. Geophys. Res., 97,* B8, 11905-1191.

RICHARDSON, R.M., 1992. Ridge forces, absolute plate motions, and the intraplate stress field. *J. Geophys. Res., 97,* B8, 11739-11748.

Alexei Nikolaev[1] and Vsevolod Nikolaev[2]

[1] *Research and Coordinating Center for Seismology and Engineering RAS, Nikoloyamskaya 51, Moscow, Russia*

[2] *Institute of Physics of the Earth RAS, B.Gruzinskaya 10, Moscow, Russia*